ORIGINAL ARTICLE

Real time FFT identification based time-varying chatter frequency mitigation in thin-wall workpiece milling

Chenxi Wang[1] · Xingwu Zhang[1] · Xuefeng Chen[1]

Abstract

Due to the detrimental effect on tool life, material removal efficiency, and workpiece surface equality, chatter has become a major obstacle to high-performance milling. According to the previous research, the active noise equalizer (ANE) can decrease chatter frequencies with having a little influence on normal frequencies, which satisfies the initial control requirement for optimization of actuator performance. Recent researches show that chatter frequencies are time-varying with broadband characteristic in thin-walled component milling. However, tradition studies focused on invariant line spectrum chatter frequency suppression, which cannot meet the time-varied need. To this end, in this research, the real-time fast Fourier transform (FFT) identification is introduced into ANE, which can update the reference chatter frequencies for time-varying chatter frequencies' suppression in thin-walled workpiece milling. However, during the period between two FFT, the identified frequencies remain unchanged, which will deviate from the real chatter frequencies and disable the controller. In order to deal with this problem, the modified narrowband filtered-x least mean square (NFXLMS) is combined with the real-time FFT identification for time-varying chatter frequencies suppression. The modified NFXLMS is a narrowband active control algorithm, which can handle the small change of chatter frequencies during the period between two FFT. Simulation results show that the proposed two control algorithms can both suppress the time-varying chatter frequencies effectively. The modified NFXLMS has better control effect than ANE, but it has larger impacts every time the chatter frequencies are identified by FFT. Finally, the thin-wall workpiece milling tests are implemented. The off-line simulation based on practical experimental data is carried out that indicates that the developed algorithms work well in practice.

Abbreviations

D	The diameter of milling tool
c_x, c_y	The modal damping in the x and y directions
f_t	The feed per tooth
F_x, F_y	The milling force in the x and y directions
$h_j(z,t)$	The instantaneous uncut chip thickness
k_x, k_y	The modal stiffness in the x and y directions
K_t, K_n	The tangential and radial shearing force coefficients
K_{te}, K_{ne}	The tangential and radial ploughing force coefficients
m_x, m_y	The modal mass in the x and y directions
N	The tooth number
Ω	The spindle speed
$\phi_j(z,t)$	The angular position of the jth tooth at the zth axial disk
ϕ_{st}, ϕ_{ex}	The start and exit angles of the cutter tooth
γ	The helix angle
$x_a(n), x_b(n)$	The reference signals defined by reference chatter frequencies
$w_a(n), w_b(n)$	The coefficient vector of controller
β	The gain factor
$e(n), e_s(n)$	The error signal
$d(n)$	The primary vibration signal through primary path

✉ Xingwu Zhang
xwzhang@mail.xjtu.edu.cn

1 State Key Laboratory for Manufacturing System Engineering, School of Mechanical Engineering, Xi'an Jiaotong University, Xi'an 710049, People's Republic of China

| $s(n)$ | The impulse response function between actuators and tooltip |
| μ_l, μ_ω | The convergence factor of adaptive algorithm |

1 Introduction

Due to the high productivity and flexibility, high-speed milling (HSM) has been widely adopted in aerospace and automobiles industry [1]. However, owing to the detrimental effect on tool life, material removal efficiency, and workpiece surface equality, chatter has become a major obstacle to high performance milling [2]. In order to remove this obstacle, more and more scholars are attracted in chatter avoidance or suppression. In general, the methods for chatter avoidance or mitigation are mainly divided into three categories, including stability prediction, passive control, and active control [2–4].

Stability analysis can provide the guidance for selection of milling parameters (spindle speed and axial cutting depth). The present study aims to obtain the stability lobe diagram (SLD) more quickly and accurately. On the one hand, lots of methods and their improved methods are proposed to acquire the SLD. For instance, Altintas et al. put forward the zero-order approximation method [5] and the multi-frequency method [6] in frequency domain. The former is the most efficient method, but cannot be applicable for small radial cutting depth. The latter is suitable to low-immersion milling, but time-consuming due to the higher-order items' approximation. As to the time domain, many discretization methods are developed. For example, the semi discretization method [7] and its higher-order methods [8] have been a popular method for a long time. Unfortunately, the matrix exponential function in SDM depends on both spindle speed and axial cutting depth, which would increase the calculation and lead to low efficiency. The full discretization method [9] constructs the Floquet matrix through direct integration and linear interpolation, where the matrix exponential function is just related with spindle speed. Besides the discretization strategies, the temporal finite element analysis is also developed for milling stability analysis with high accuracy and efficiency [10]. On the other hand, lots of researchers try to obtain the SLD as accurately as possible, through considering practical factors, such as helix angle [11, 12], runout [13], process damping [14], tool deflection [12, 15], thin-walled workpiece [16], and material removal [17, 18]. However, this method cannot expand the stability zone of SLD. However, the accurate prediction of SLD can just guide for cutting parameter selection; however, it cannot guarantee that the cutting parameters remain constant and the original stable system may lose stabilization owing to the time-varying property of cutting process [19].

The passive control technique attempted to suppress chatter by changing the system behavior, which is based on improving the design of the machine tool to change its performance against vibration (variable pitch [20] or variable helix [21]) or on the use of extra devices (tuned mass damper [22]) that can absorb extra energy or disrupt the regenerative effect. However, due to the time-varying property and uncertainty of cutting process, the passive control cannot show good performance without extra energy input [23, 24].

As the third strategy, active control is an effective method for chatter suppression, which can satisfy the real-time requirements of the online control system and realize high-performance and high-efficiency cutting. Different actuators can be integrated into spindle, such as electrostrictive actuator [18], active magnetic bearing [19], and piezoelectric stack [20, 21]. With extra energy input, the active control system is able to change the dynamics property of machine tool and afford additional forces for chatter suppression, so that the stable cutting region can be expanded. For example, Niels and Verschuren [25] adopted the robust active control method for chatter suppression, which can guarantee the robust stability. Monnin et al. [26, 27] adopted the optimal control algorithm for chatter suppression using active spindle equipped with piezoelectric stacks. Using piezoelectric patch as the actuator, Zhang et al. [24] applied LMS active control method to milling process and suppress chatter vibration energy almost by 50%.

The traditional active chatter control algorithm takes the vibration signals in time domain as the feedback signals, which will suppress all the vibration frequencies, including both chatter frequencies and normal frequencies. Therefore, actuators in traditional control strategies have to waste much energy for rotation frequency and its frequency multiplications, which cannot obtain the optimal performance and cause the saturation effect of actuators. In order to solve this problem, Wang et al. [23] adopted the adaptive vibration reshaping algorithm for line spectrum control, which can suppress chatter frequencies effectively without changing rotation frequency and its frequency multiplications. However, this algorithm is just suitable to the condition where chatter frequencies keep unchanged. On the basis of researches [28–30], chatter frequencies vary in thin-walled workpiece milling.

In order to suppress time-varying chatter frequencies, this research introduced the real-time FFT identification into ANE [23] and modified NFXLMS [31]. ANE can suppress chatter frequencies effectively without changing rotation frequency and its frequency multiplications; however, it is sensitive to the chatter frequencies' identification errors. With the chatter frequencies' identification errors increasing, the controller performance decreases until fail. Therefore, the real-time FFT identification can modify the identified reference frequencies for better controller performance. However,

if the real-time FFT identification is implemented at every step, it will increase the calculation burden of controller and the control delay, which will decrease the controller performance a lot [23]. Thus, in this research, the real-time FFT identification is implemented at every N steps, where N depends on the convergence factors [12]. In that case, a new problem arises; that is, chatter frequencies vary during the N steps. Hence, the modified NFXLMS is adopted to replace ANE, where the reference frequencies can be updated iteratively by a new adaptive algorithm during two chatter frequencies identifications by FFT. Simulation results show that the modified NFXLMS has better control effect than ANE.

The remainder of this paper is arranged as follows. In Sect. 2, the time-varying chatter frequencies phenomenon is introduced and verified by milling tests. Section 3 presents the chatter suppression algorithm based on ANE and modified NFXLMS with FFT. Besides, the numerical simulation is provided. In Sect. 4, the measured vibration data in thin-wall workpiece milling is applied for algorithm verification. Finally, some conclusions and future works are drawn in Sect. 5.

2 The time-varying chatter frequencies phenomenon in thin-walled workpiece milling

As seen in Fig. 1, the milling tool is usually assumed to be rigid in thin-walled part milling [32, 33]. Then, the governing equation can be expressed by:

$$\begin{bmatrix} m_x & 0 \\ 0 & m_y \end{bmatrix} \begin{bmatrix} \ddot{x}(t) \\ \ddot{y}(t) \end{bmatrix} + \begin{bmatrix} c_x & 0 \\ 0 & c_y \end{bmatrix} \begin{bmatrix} \dot{x}(t) \\ \dot{y}(t) \end{bmatrix} + \begin{bmatrix} k_x & 0 \\ 0 & k_y \end{bmatrix} \begin{bmatrix} x(t) \\ y(t) \end{bmatrix} = \begin{bmatrix} F_x(t) \\ F_y(t) \end{bmatrix}$$
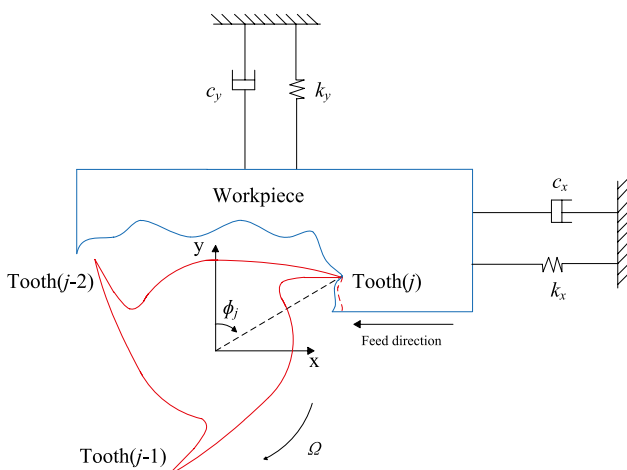(1)

Fig. 1 The schematic representation of the milling process

where $\begin{bmatrix} m_x & 0 \\ 0 & m_y \end{bmatrix}$, $\begin{bmatrix} c_x & 0 \\ 0 & c_y \end{bmatrix}$, and $\begin{bmatrix} k_x & 0 \\ 0 & k_y \end{bmatrix}$ are the modal mass, modal damping, and modal stiffness matrixes of the thin-walled components, respectively; $[F_x(t) F_y(t)]^T$ and $[x(t) y(t)]^T$ are the milling forces and vibration displacement vectors in the x and y directions.

To calculate the instantaneous milling forces, the tool is discretized into N_a axial disk layers with $dz = a_p/N_a$, where a_p is the axial milling depth and dz is the height of each axial discretization disk. Hence, the milling forces can be written as follows:

$$\begin{bmatrix} F_x(t) \\ F_y(t) \end{bmatrix} = \sum_{z=1}^{Na} \sum_{j=1}^{N} \begin{bmatrix} -\cos(\phi_j(z,t)) & -\sin(\phi_j(z,t)) \\ -\sin(\phi_j(z,t)) & -\cos(\phi_j(z,t)) \end{bmatrix} \left\{ \begin{bmatrix} K_t \\ K_n \end{bmatrix} h_j(z,t) + \begin{bmatrix} K_{te} \\ K_{ne} \end{bmatrix} \right\} g(\phi_j(z,t)) dz$$
(2)

where N is the number of teeth; K_t and K_n are the tangential and radial shearing force coefficients; K_{te} and K_{ne} are the tangential and radial ploughing force coefficients; and $g(\phi_j(z,t))$ is a switch function for determining whether the tooth is in or out of cut, which can be expressed as $\begin{cases} g(\phi_j(z,t)) = 1 & \phi_{st} < \phi_j(z,t) < \phi_{ex} \\ g(\phi_j(z,t)) = 0 & otherwise \end{cases}$, where ϕ_{st} and ϕ_{ex} are the start and exit angles of the cutter tooth.

$\phi_j(z,t)$ is the angular position of the jth tooth at the zth axial disk, which can be given by:

$$\phi_j(z,t) = (2\pi\Omega/60)t + (j-1) \cdot 2\pi/N - 2z\tan\gamma/D$$
(3)

where Ω, γ, and D are the spindle speed (in rpm), helix angle, and diameter of milling tool, respectively.

The instantaneous uncut chip thickness $h_j(z,t)$ can be obtained as follows:

$$h_j(z,t) = f_t\sin(\phi_j(z,t)) + \Delta x_{jz}\sin(\phi_j(z,t)) + \Delta y_{jz}\cos(\phi_j(z,t))$$
(4)

where f_t is the feed per tooth (in mm/tooth); Δx_{jz} and Δy_{jz} are the instantaneous uncut chip thickness of the jth tooth at the zth axial disk in the x and y directions, respectively.

The modal parameters are usually obtained by finite element analysis or experiment modal analysis. In thin-walled workpiece milling, the corresponding modal parameters are time-varying with the workpiece material removal and the change of tool position, which will cause the variation of chatter frequencies [30]. The detailed description about milling forces can refer to the literature [33]. The dominant chatter frequencies can be calculated with the developed theory in [34]. Similar as Fig. 2, the experimental results in [18, 28–30] have verified the existence of the time-varying chatter frequencies phenomenon. For the small-sized thin-walled part in milling tests, the chatter frequency varies from 225 to 220 Hz.
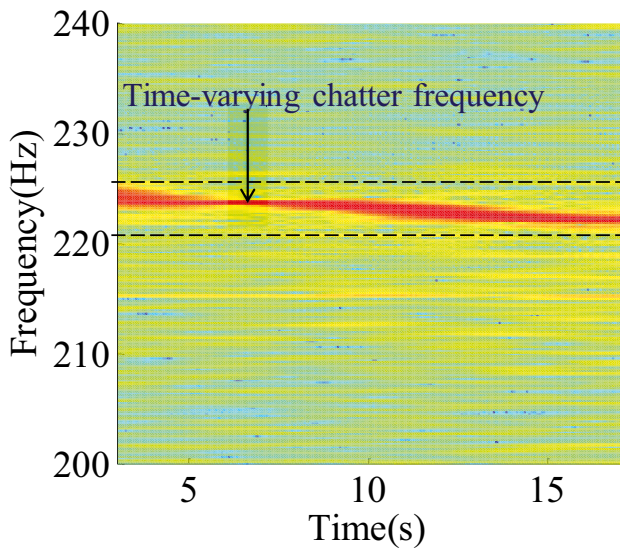
Fig. 2 The time-varying plane of acceleration signals in thin-walled workpiece milling

For the implementation of the successive control algorithm in time domain, the Euler approximation method [35] is adopted to solve the milling dynamic equation numerically to investigate the dynamic behavior under a specific cutting condition:

$$\ddot{x}(t_i) = \frac{F_x(t_i) - c_x\dot{x}(t_i) - k_x x(t_i)}{m_x}, \ddot{y}(t_i) = \frac{F_y(t_i) - c_y\dot{y}(t_i) - k_y y(t_i)}{m_y} \tag{5}$$

$$\dot{x}(t_i) = \dot{x}(t_{i-1}) + \ddot{x}(t_i)dt, \dot{y}(t_{i-1}) + \ddot{y}(t_i)dt \tag{6}$$

$$x(t_i) = x(t_{i-1}) + \dot{x}(t_i)dt, y(t_i) = y(t_{i-1}) + \dot{y}(t_i)dt \tag{7}$$

where i is an integer number starting from one and dt is the time step. The time domain simulation results have been verified by the stability lobe diagram [23] and milling tests [36], which can be used for control algorithm simulation verification in the following sections.

3 Real-time FFT identification-based time-varying chatter frequency mitigation

3.1 Real-time FFT identification-based ANE

In order to elaborate the control block diagram conveniently, some explanations for Figs. 3 and 4 are listed as follows: The transfer function $P(n)$ is the tooltip impulse response function. The transfer function $S(n)$ is the impulse response function between actuators and tooltip. The red lines and blocks are in physical domain, which are realized by hardware in control process. The black lines and blocks are in electrical domain, which are realized by programs. is the adder in physical domain; is the logical adder in electrical domain.

The ANE based on real-time FFT identification is presented in Fig. 3. Compared with the classical ANE control (Fig. 2 in [23]), this research adds the FFT identification every N steps in the diagram. As for the detailed description, please refer to the literature [23]. Here, just summarize the ANE algorithm as follows:

$$\begin{cases} \boldsymbol{x}_a(n) = \cos(\boldsymbol{\Omega}n), \boldsymbol{x}_b(n) = \sin(\boldsymbol{\Omega}n) \\ y(n) = \boldsymbol{w}_a^{\mathrm{T}}(n)\boldsymbol{x}_a(n) + \boldsymbol{w}_b^{\mathrm{T}}(n)\boldsymbol{x}_b(n) \\ y_c(n) = (1-\beta)y(n), y_b(n) = \beta y(n) \\ e(n) = d(n) - y_c(n) * s(n) \\ e_s(n) = d(n) - y_b(n) * s(n) \\ \boldsymbol{w}_l(n+1) = \boldsymbol{w}_l(n) + \mu_l e_s(n)\left[\boldsymbol{x}_l(n) * s(n)\right], (l=a,b) \end{cases} \tag{8}$$
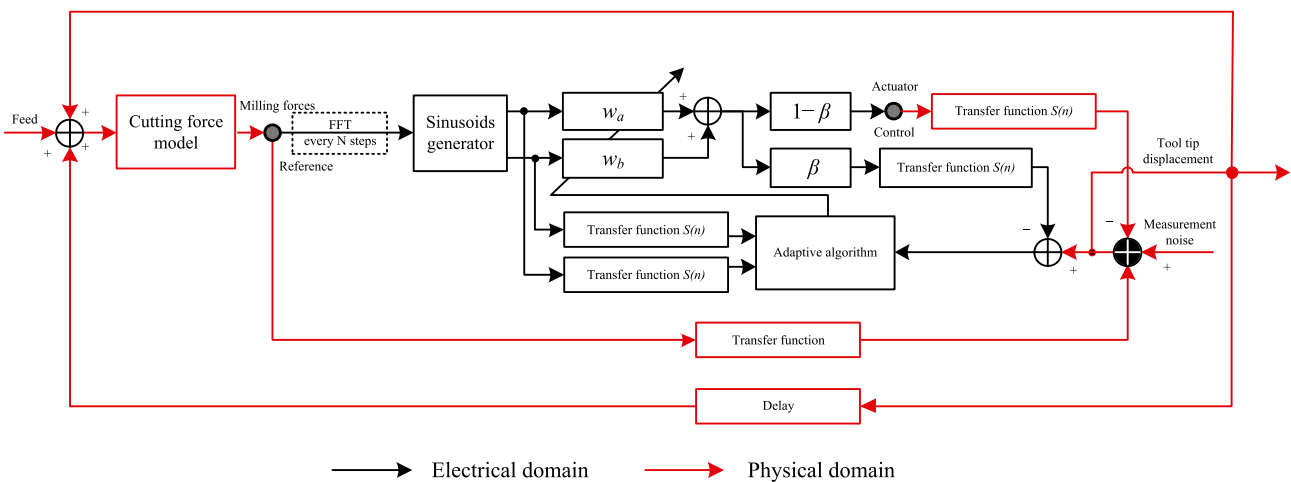

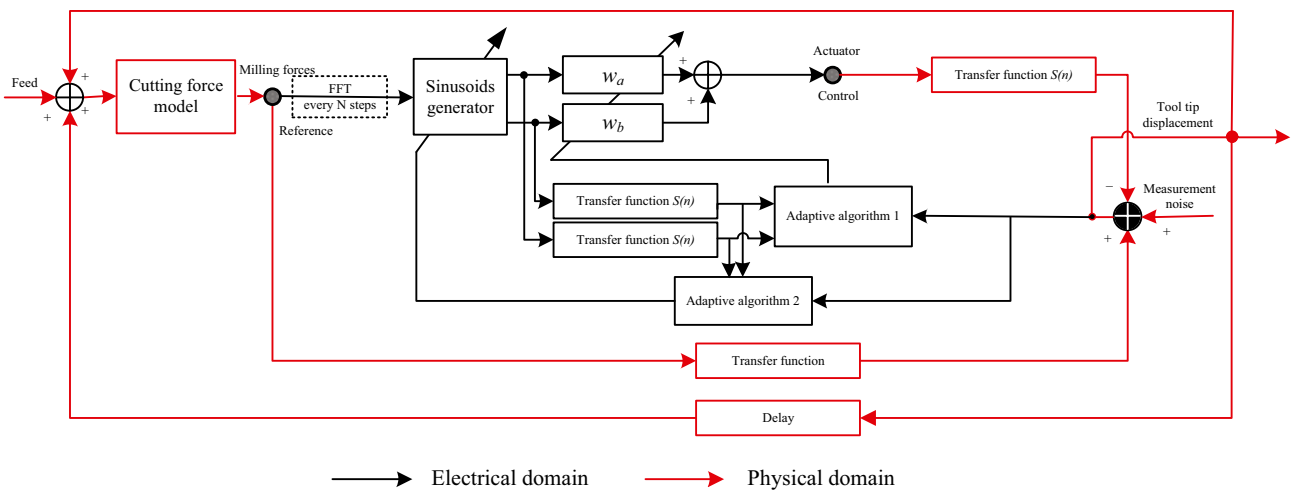**Fig. 3** The block diagram with ANE based on real-time FFT identification

Fig. 4 The block diagram with modified NFXLMS based on real-time FFT identification

3.2 Real-time FFT identification-based modified NFXLMS

The modified NFXLMS based on real-time FFT identification is presented in Fig. 4. Compared with Fig. 3, it adds another adaptive algorithm to update the reference frequencies during two chatter frequency identifications by FFT. The detailed derivation is as follows [31].

The output of controller can be expressed by:

$$y(n) = \mathbf{w}_a^{\mathrm{T}}(n)\mathbf{x}_a(n) + \mathbf{w}_b^{\mathrm{T}}(n)\mathbf{x}_b(n) \tag{9}$$

where $\mathbf{w}_l(n), l = a, b$ is the coefficient vector of controller; $\mathbf{x}_a(n)$ and $\mathbf{x}_b(n)$ are the reference signals defined by reference chatter frequencies. The error signal can be written as follows:

$$e(n) = d(n) - y(n) * s(n) \tag{10}$$

where $d(n)$ is the primary vibration signal through primary path; $s(n)$ is the impulse response function between actuators and tooltip.

The reference signals from sinusoids generator can be written as follows:

$$\mathbf{x}_l(n) = 2\cos\mathbf{\Omega}_r \cdot \mathbf{x}_l(n-1) - \mathbf{x}_l(n-2), (l = a, b) \tag{11}$$

where:

$$\cos\mathbf{\Omega}_r \equiv \mathrm{diag}\big[\cos\boldsymbol{\omega}_r\big] \tag{12}$$

where $\boldsymbol{\omega}_r$ is the identified reference signal frequency.

Substituting Eq. (11) into Eqs. (9) and (10) leads to:

$$\begin{aligned} e(n) =& d(n) - \big[2\mathbf{w}_a^T(n)\cos\mathbf{\Omega}_r \cdot \mathbf{x}_a(n-1) + 2\mathbf{w}_b^T(n) \\ & \cos\mathbf{\Omega}_r \cdot \mathbf{x}_b(n-1) - \mathbf{w}_a^T(n)\mathbf{x}_a(n-2) - \mathbf{w}_b^T \\ & (n)\mathbf{x}_b(n-2)\big] * s(n) \end{aligned} \tag{13}$$

It can be seen that the residual error is a non-linear function of the reference frequencies due to the nonlinear function $\cos\mathbf{\Omega}_r$. Through the steepest descent method, the updating equation of the reference frequencies can be expressed by:

$$\mathbf{\Omega}_r(n+1) = \mathbf{\Omega}_r(n) + \frac{\mu_\omega}{2}\frac{\partial e^2(n)}{\partial\mathbf{\Omega}_r} \tag{14}$$

where μ_ω is the convergence factor of adaptive algorithm 2 and the gradient is as follows:

$$\frac{\partial e^2(n)}{\partial\mathbf{\Omega}_r} = \sin\mathbf{\Omega}_r\big[\mathbf{Y}(n)\hat{*s}(n)\big]e(n) \tag{15}$$

where:

$$\mathbf{Y}(n) = \big[\mathbf{w}_a(n)\mathbf{x}_a^T(n-1) + \mathbf{w}_b(n)\mathbf{x}_b^T(n-1)\big] \tag{16}$$

where $\hat{s}(n)$ is the identified model of $s(n)$.

Then, summarize the NFXLMS algorithm as follows:

$$\begin{cases} \mathbf{x}_a(n) = 2\cos\mathbf{\Omega}_r(n)\mathbf{x}_a(n-1) - \mathbf{x}_a(n-2) \\ \mathbf{x}_b(n) = 2\cos\mathbf{\Omega}_r(n)\mathbf{x}_b(n-1) - \mathbf{x}_b(n-2) \\ y(n) = \mathbf{w}_a^T(n)\mathbf{x}_a(n) + \mathbf{w}_b^T(n)\mathbf{x}_b(n) \\ e(n) = d(n) - y(n) * s(n) \\ \mathbf{w}_l(n+1) = \mathbf{w}_l(n) + \mu_l e(n)\big[\mathbf{x}_l(n) * \hat{s}(n)\big], (l = a, b) \\ \mathbf{\Omega}_r(n+1) = \mathbf{\Omega}_r(n) + \mu_\omega\sin\mathbf{\Omega}_r\big[\mathbf{Y}(n) * \hat{s}(n)\big]e(n) \end{cases} \tag{17}$$

3.3 Numerical simulation for time-varying chatter frequency suppression

In order to verify the proposed algorithm, numerical simulation is implemented in this section. The milling parameters are presented in Table 1 with spindle speed 7500 rpm and

Table 1 The time domain simulation parameters

Simulation parameters	Value
Tool teeth number	4
Tangential cutting force coefficient (N/m^2)	7e8
Normal cutting force coefficient (N/m^2)	2.1e8
Tangential edge constant (N/m^2)	4000
Normal edge constant (N/m^2)	3000
Feed per tooth (m/tooth)	1e-4
Tool diameter (m)	0.019
Helix angle (°)	30
Modal mass in the x direction (kg)	0.5629
Modal mass in the y direction (kg)	0.4613
Modal damping in the x direction	0.03
Modal damping in the y direction	0.025
Modal stiffness in the x direction (N/m)	8e6
Modal stiffness in the y direction (N/m)	7e6
Milling type	Up-milling
Radial milling depth (m)	0.0152

axial cutting depth 1 mm. In milling process, the stiffness of thin-wall workpiece change by 4%, which will cause time-varying chatter frequencies [30]. The controller parameters in control process are as follows. The convergence factors of ANE are 0.0015 and 0.001 in the x and y directions, respectively. The convergence factors of two adaptive algorithms in modified NFXLMS are 0.014 and 0.05.

Figure 5 gives the vibration displacement in time domain with ANE control based on FFT. For comparison, the simulation result without FFT is also presented. Results show that ANE with FFT keeps normal working condition, while the controller performance without FFT decreases until fails. The vibration displacement in frequency domain for

the whole cutting process and the stable control time are presented in Figs. 6 and 7, respectively, which display that time-varying chatter frequencies are suppressed while normal chatter frequencies are not influenced.

Figure 8 gives the vibration displacement in time domain with modified NFXLMS based on FFT. For comparison, the simulation result with ANE based on FFT is also presented. Results show that the modified NFX-LMS has better control effect than ANE. The vibration displacement in frequency domain for the whole cutting process and the stable control time are presented in Fig. 9 and Fig. 10, respectively, which display that time-varying chatter frequencies are suppressed while normal chatter frequencies are hardly influenced and the modified NFX-LMS based on FFT has better control results. In addition, the iteratively updated reference frequencies in modified NFXLMS are also provided Fig. 11, which shows that the reference frequencies vary during two chatter frequency identifications by FFT.

4 Case study using experimental data

In order to verify the proposed algorithm, the measured data in Sect. 2 is used to off-line simulation. The detailed description about set-up and experimental parameters can refer the literature [30]. The calculation results are given in Fig. 12, 13, 14, 15, 16, 17. These figures indicate that, with two developed algorithms, the time-varying chatter frequencies (marked with numbers) are suppressed while normal frequencies keep unchanged. The off-line simulation using experimental data displays that the proposed algorithm can suppress the time-varying chatter frequencies with no influence on normal frequencies.

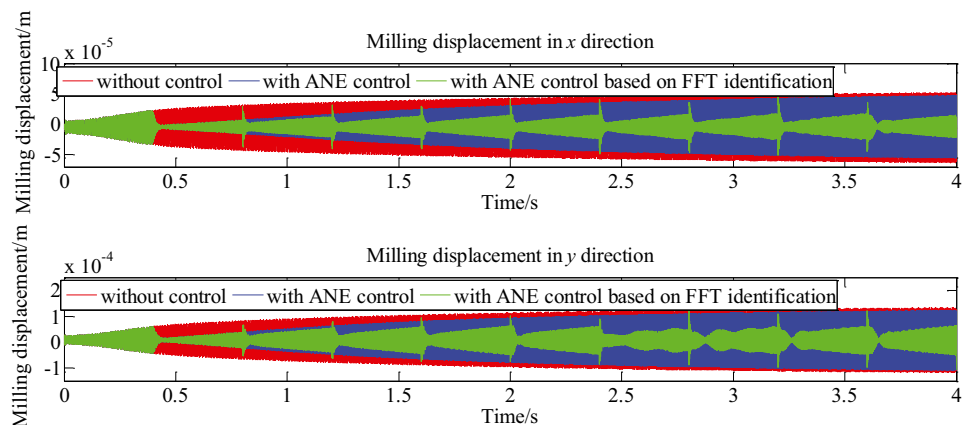**Fig. 5** The vibration displacement in time domain with ANE control based on FFT

Fig. 6 The vibration displacement in frequency domain with ANE control based on FFT for the whole cutting process
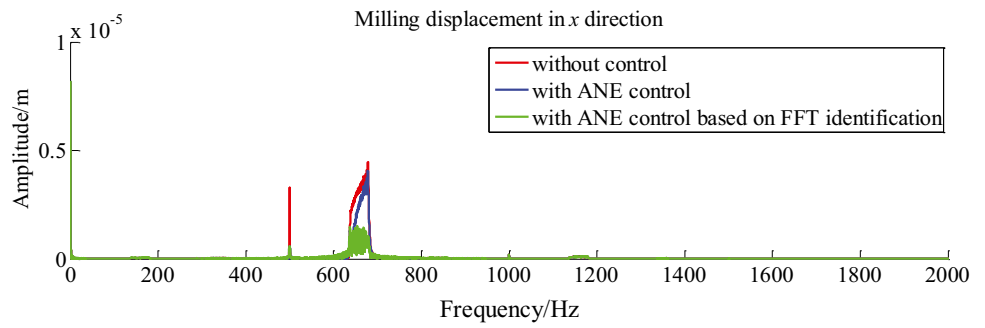

Fig. 7 The vibration displacement in frequency domain with ANE control based on FFT for the stable control time
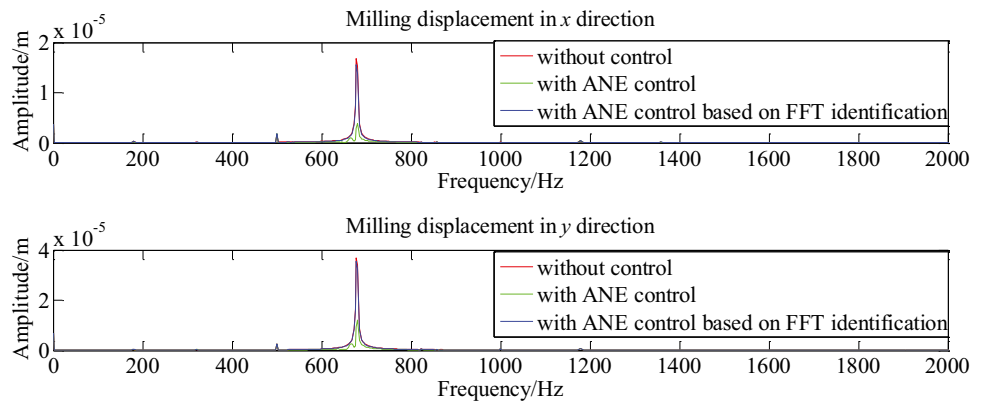

Fig. 9 The vibration displacement comparison under ANE and NFXLMS control in frequency domain for the whole cutting process
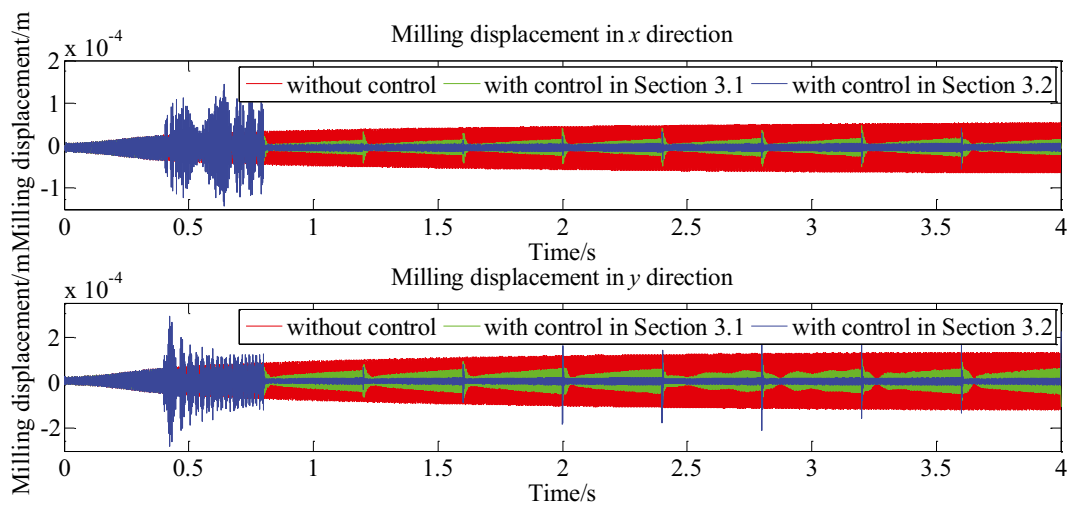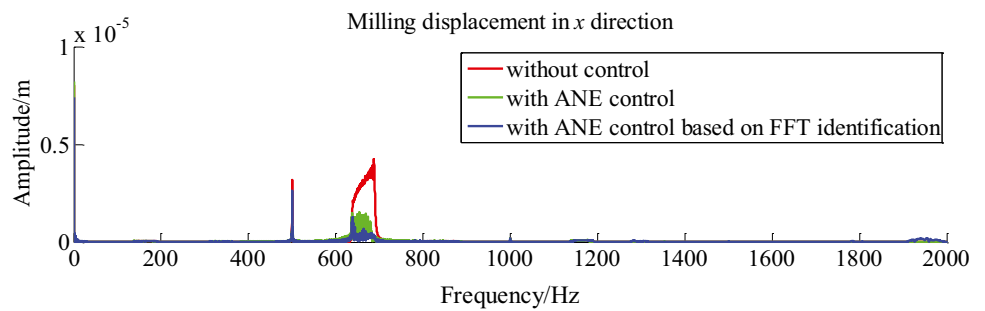

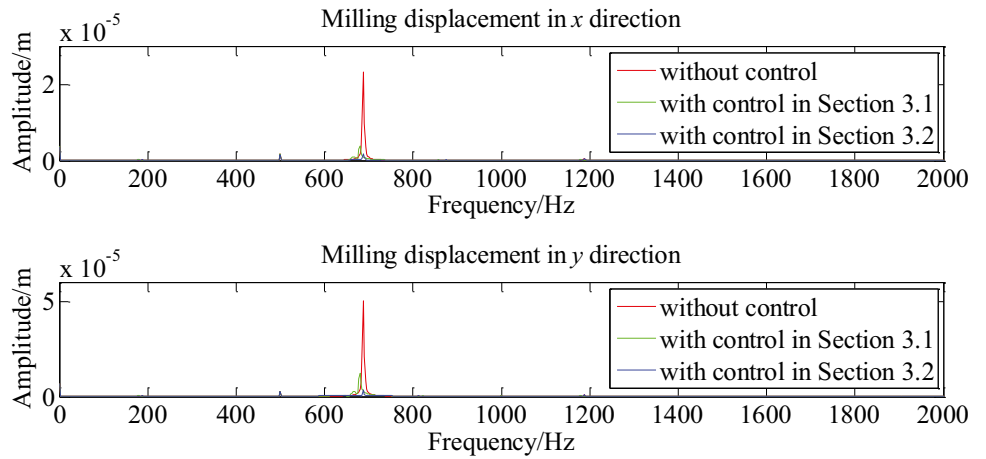
Fig. 8 The vibration displacement comparison under ANE and NFXLMS control in time domain

Fig. 10 The vibration displacement comparison under ANE and NFXLMS control in frequency domain for the stable control time

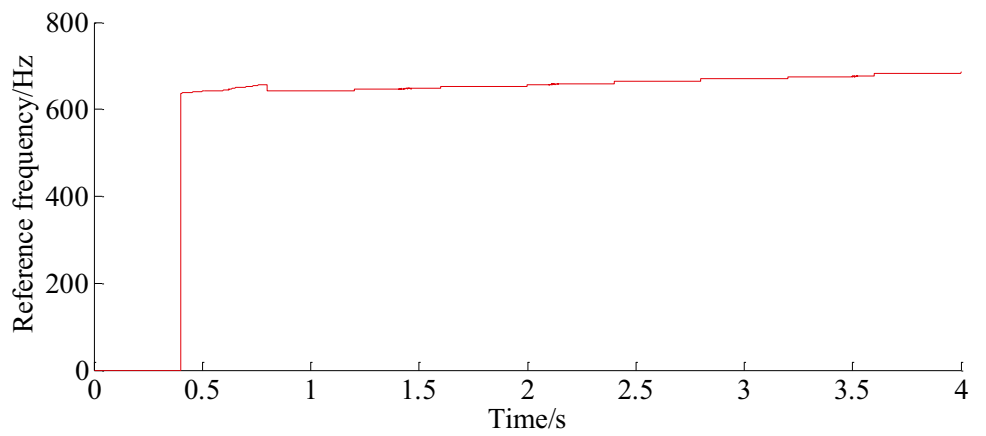**Fig. 11** The iteratively updated reference frequencies in modified NFXLMS

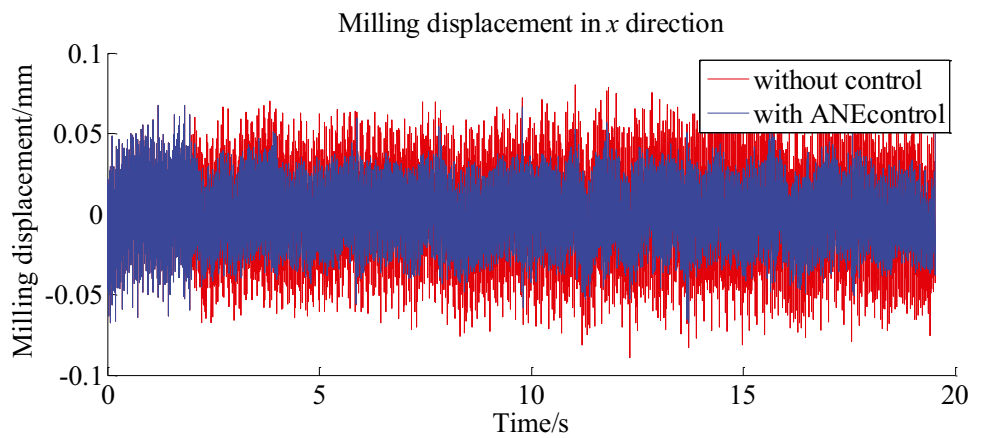**Fig. 12** The vibration signals with ANE control based on FFT

Fig. 13 The vibration signal in frequency domain with ANE control based on FFT for the whole cutting process
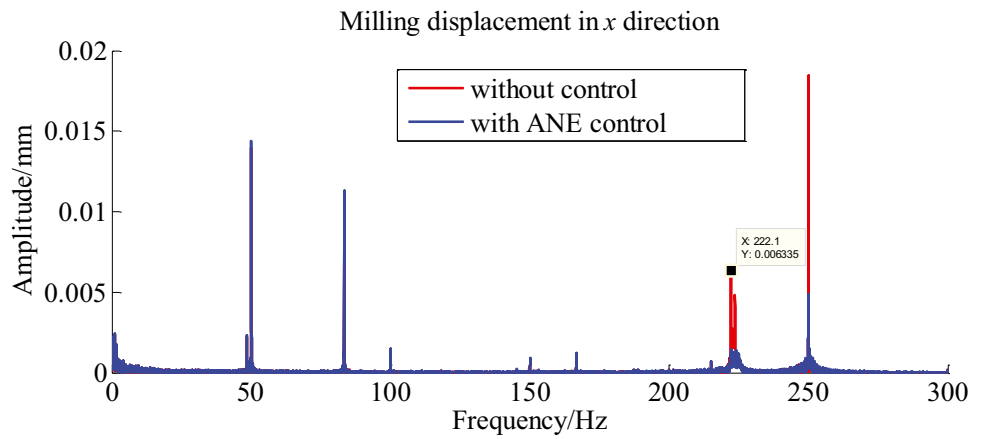

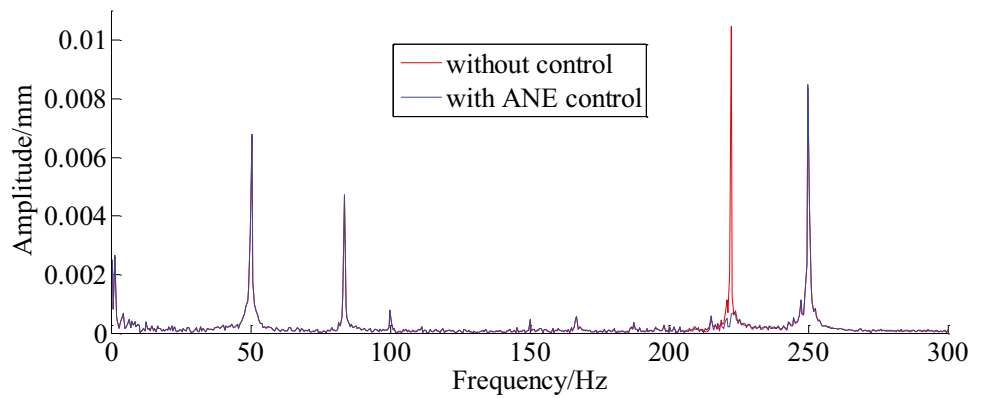**Fig. 14** The vibration signal in frequency domain with ANE control based on FFT for the stable control time

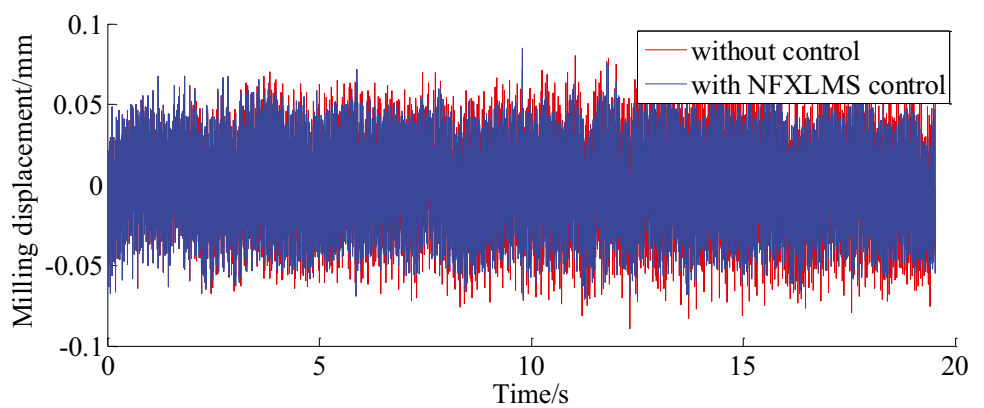**Fig. 15** The vibration signals with NFXLMS control based on FFT

Fig. 16 The vibration signal in frequency domain with NFX-LMS control based on FFT for the whole cutting process
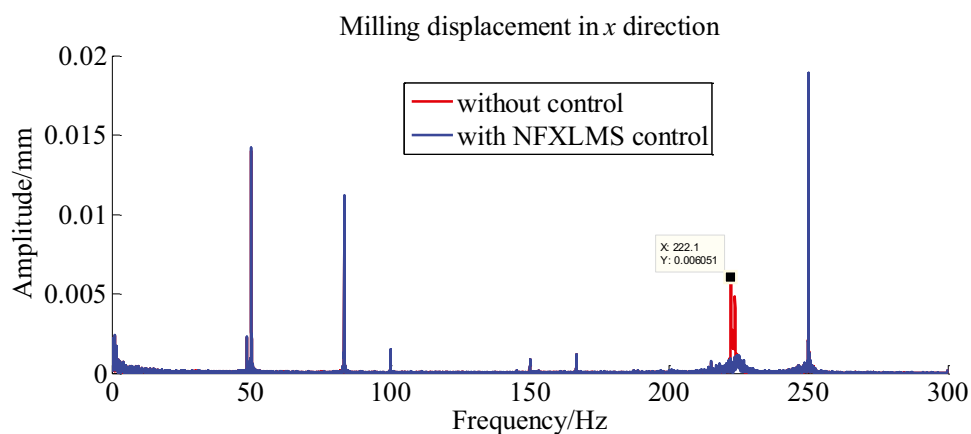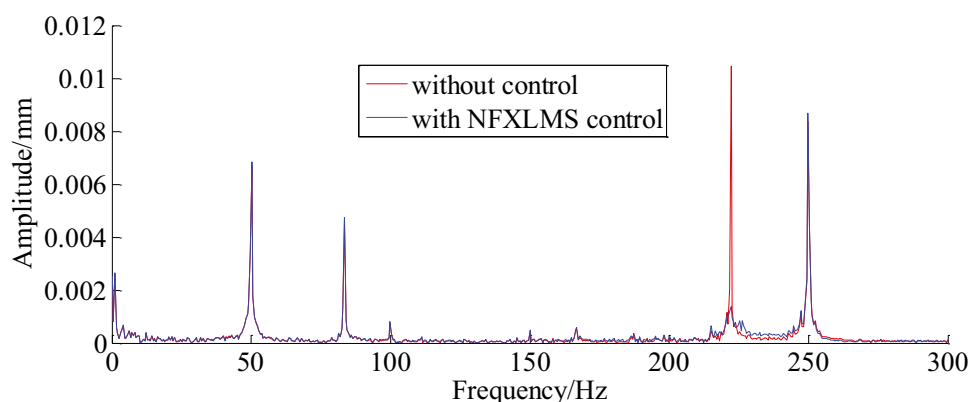

Fig. 17 The vibration signal in frequency domain with NFX-LMS control based on FFT for the stable control time

5 Conclusions

In this research, the real-time FFT identification is introduced into ANE and modified NFXLMS for time-varying chatter frequencies suppression in thin-walled workpiece milling. Simulation results show that the proposed two control algorithms can both suppress the time-varying chatter frequencies effectively. The modified NFXLMS has better control effect than ANE, but it has larger impacts every time the chatter frequencies are identified by FFT, which is harmful to part surface quality. Finally, the off-line simulation based on practical experimental data is implemented that indicates that the developed algorithms work well in practice. In this research, the chatter frequency identification based on FFT is not continuous; therefore, the continuous chatter frequencies tracking algorithm need to be developed for time-varying chatter detection and mitigation in the future.

Data availability The data that support the findings of this study are available on request.

Code availability Code can be partially shared upon request.

Declarations

Ethics approval The authors confirm that they have abided to the publication ethics and state that this work is original and has not been used for publication anywhere before. No ethical approval required for the experiments conducted.

Consent to participate The authors hereby consent to participate.

Consent for publication The authors hereby consent to the publication of the proposed manuscript in JAMT.

Competing interests The authors declare no competing interests.

References

1. Cao H, Zhang X, Chen X (2017) The concept and progress of intelligent spindles: a review. Int J Mach Tools Manuf 112:21–52

2. Quintana G, Ciurana J (2011) Chatter in machining processes: a review. Int J Mach Tools Manuf 51(5):363–376

3. Siddhpura M, Paurobally R (2012) A review of chatter vibration research in turning. International Journal of Machine tools manufacture 61:27–47

4. Wang C, Zhang X, Liu Y, Cao H, Chen X (2018) Stiffness variation method for milling chatter suppression via piezoelectric stack actuators. Int J Mach Tools Manuf 124:53–66

5. Altintas Y, Budak E (1995) Analytical prediction of stability lobes in milling. CIRP Ann 44(1):357–362

6. Merdol SD, Altintas Y (2004) Multi frequency solution of chatter stability for low immersion milling. J Manuf Sci Eng 126(3):459–466

7. Insperger T, Stépán G (2004) Updated semi-discretization method for periodic delay-differential equations with discrete delay. Int J Numer Meth Eng 61(1):117–141

8. Insperger T, Stépán G (2011) Semi-discretization for time-delay systems: stability and engineering applications, vol 178. Springer Science & Business Media

9. Ding Y, Zhu L, Zhang X, Ding H (2010) A full-discretization method for prediction of milling stability. Int J Mach Tools Manuf 50(5):502–509

10. Bayly PV, Halley JE, Mann BP, Davies MA (2003) Stability of interrupted cutting by temporal finite element analysis. J Manuf Sci Eng 125(2):220–225

11. Lin Z, Huang X, Akhtar MM (2011) Chatter stability of low-immersion milling in multi-frequency with helix angle. Adv Sci Lett 4(6–7):2076–2081

12. Wang C, Zhang X, Cao H, Chen X, Xiang J (2018) Milling stability prediction and adaptive chatter suppression considering helix angle and bending. The International Journal of Advanced Manufacturing Technology 95(9–12):3665–3677

13. Niu J, Ding Y, Geng Z, Zhu L, Ding H (2018) Patterns of regenerative milling chatter under joint influences of cutting parameters, tool geometries, and runout. J Manuf Sci Eng 140(12):121004

14. Ahmadi K, Ismail F (2011) Analytical stability lobes including nonlinear process damping effect on machining chatter. Int J Mach Tools Manuf 51(4):296–308

15. Totis G, Albertelli P, Torta M, Sortino M, Monno M (2017) Upgraded stability analysis of milling operations by means of advanced modeling of tooling system bending. J International Journal of Machine Tools Manufacture 113:19–34

16. Aslan D, Altintas Y (2018) On-line chatter detection in milling using drive motor current commands extracted from CNC. Int J Mach Tools Manuf 132:64–80

17. Dang X-B, Wan M, Yang Y, Zhang W-H (2019) Efficient prediction of varying dynamic characteristics in thin-wall milling using freedom and mode reduction methods. Int J Mech Sci 150:202–216

18. Wan M, Dang X-B, Zhang W-H, Yang Y (2018) Optimization and improvement of stable processing condition by attaching additional masses for milling of thin-walled workpiece. Mech Syst Signal Process 103:196–215

19. Wang C, Zhang X, Liu J, Yan R, Cao H, Chen X (2019) Multi harmonic and random stiffness excitation for milling chatter suppression. Mech Syst Signal Process 120:777–792

20. Iglesias A, Dombovari Z, Gonzalez G, Munoa J, Stepan G (2019) Optimum selection of variable pitch for chatter suppression in face milling operations. Materials 12(1):112

21. Otto A, Rauh S, Ihlenfeldt S, Radons G (2017) Stability of milling with non-uniform pitch and variable helix tools. The International Journal of Advanced Manufacturing Technology 89(9–12):2613–2625

22. Burtscher J, Fleischer J (2017) Adaptive tuned mass damper with variable mass for chatter avoidance. CIRP Ann 66(1):397–400

23. Wang C, Zhang X, Liu J, Cao H, Chen X (2019) Adaptive vibration reshaping based milling chatter suppression. Int J Mach Tools Manuf 141:30–35

24. Zhang X, Wang C, Gao R, Yan R, Chen X, Wang S (2016) A novel hybrid error criterion-based active control method for on-line milling vibration suppression with piezoelectric actuators and sensors. Sensors 16(1):68

25. van Dijk NJ, van de Wouw N, Doppenberg EJ, Oosterling HA, Nijmeijer H (2011) Robust active chatter control in the high-speed milling process. IEEE Trans Control Syst Technol 20(4):901–917

26. Monnin J, Kuster F, Wegener K (2014) Optimal control for chatter mitigation in milling—part 1: modeling and control design. Control Eng Pract 24:156–166

27. Monnin J, Kuster F, Wegener K (2014) Optimal control for chatter mitigation in milling—part 2: experimental validation. Control Eng Pract 24:167–175

28. Yang Y, Zhang W-H, Ma Y-C, Wan M (2016) Chatter prediction for the peripheral milling of thin-walled workpieces with curved surfaces. Int J Mach Tools Manuf 109:36–48

29. Feng J, Wan M, Gao T-Q, Zhang W-H (2018) Mechanism of process damping in milling of thin-walled workpiece. Int J Mach Tools Manuf 134:1–19

30. Wang C, Zhang X, Chen X, Cao H (2019) Time-Varying chatter frequency characteristics in thin-walled workpiece milling with B-spline wavelet on interval finite element method. J Manuf Sci Eng 141(5):051008

31. Liu J, Chen X, Yang L, Gao J, Zhang X (2017) Analysis and compensation of reference frequency mismatch in multiple-frequency feedforward active noise and vibration control system. J Sound Vib 409:145–164

32. Song Q, Liu Z, Wan Y, Ju G, Shi J (2015) Application of Sherman–Morrison–Woodbury formulas in instantaneous dynamic of peripheral milling for thin-walled component. Int J Mech Sci 96:79–90

33. Liu Y, Wu B, Ma J, Zhang D (2017) Chatter identification of the milling process considering dynamics of the thin-walled workpiece. The International Journal of Advanced Manufacturing Technology 89(5–8):1765–1773

34. Dombovari Z, Iglesias A, Zatarain M, Insperger T (2011) Prediction of multiple dominant chatter frequencies in milling processes. Int J Mach Tools Manuf 51(6):457–464

35. Schmitz TL, Smith KS (2014) Machining dynamics. Springer

36. Honeycutt A, Schmitz T (2017) A numerical and experimental investigation of period-n bifurcations in milling. J Manuf Sci Eng 139(1):011003

Publisher's Note Springer Nature remains neutral with regard to jurisdictional claims in published maps and institutional affiliations.